doi:10.20944/preprints202305.0349.v1

Article

Vapor Composition and Vaporization Thermodynamics of 1-Ethyl-3-Methylimidazolium Hexafluorophosphate Ionic Liquid

Anatoliy M. Dunaev [1,*], Vladimir B. Motalov [1], Mihail A. Korobov [1],Dmitrii Govorov [2], Victor V. Aleksandriiskii[3] and Lev S. Kudin [1]

[1] *Ivanovo State University of Chemistry and Technology, Department of Physics, Ivanovo, Russia;* amdunaev@ro.ru
[2] *University of Cincinnati, Department of Chemistry, Cincinnati, Ohio, USA;* govorodi@mail.uc.edu
[3] *Ivanovo State University of Chemistry and Technology, , Department of Chemistry and Technology of High-Molecular Compounds, Ivanovo, Russia;* nmr@isuct.ru
* Correspondence: amdunaev@ro.ru

Abstract: The processes of the sublimation and thermal decomposition of the 1-ethyl-3-methylimidazolium hexafluorophosphate ionic liquid (EMImPF$_6$) were studied by a complex approach including Knudsen effusion mass spectrometry, IR and NMR spectroscopy, and quantum chemical calculations. It was established that the vapor over liquid phase primarily consists of decomposition products under equilibrium conditions. Otherwise, the neutral ion pairs are the only vapor components under Langmuir conditions. To identify the nature of the decomposition products an experiment on the distillation of the ionic liquid was performed and the collected distillate was analyzed. It was revealed by the IR and NMR spectroscopy that EMImPF$_6$ decomposes to substituted imidazole-2-ylidene ($C_6N_2H_{10}PF_5$) and HF. The measured vapor pressure of $C_6N_2H_{10}PF_5$ reveals a very low activity of the decomposition products ($<10^{-4}$) in the liquid phase. The absence of significant accumulation of decomposition products in the condensed phase makes it possible to determine the enthalpy of sublimation of the ionic liquid assuming its unchanged activity. The thermodynamics of the EMImPF$_6$ sublimation was studied by Knudsen effusion mass spectrometry. The formation enthalpy of EMImPF$_6$ in ideal gas state was found from combination of the sublimation enthalpy and formation enthalpy of ionic liquid in the condensed state. The obtained value is in good agreement with those calculated by quantum chemical methods.

Keywords: ionic liquids; imidazolium; hexafluorophosphate; Knudsen effusion mass spectrometry; quantum chemical calculations; thermodynamics; evaporation, decomposition, vapor pressure

1. Introduction

Vaporization of ionic liquids (ILs) with highly electronegative anions under high vacuum conditions is accompanied by partial decomposition of ILs with the formation of substituted imidazole-2-ylidenes. In particular, such decomposition products were clearly identified for ILs with the BF$_4^-$ [1-3], PF$_6^-$ [4], dicyanamide, thiocyanate, tricyanomethanide, and vinylogous dicyanamide anions [5]. The only exception is the work of Volpe et al. [6] where the formation of alkylimidazoles was postulated for 1-butyl-3-methylimidazolium hexafluorophosphate (BMImPF$_6$), apparently erroneously, see [3] for details. As reported in literature [1-3, 6], the competing evaporation/decomposition results in complex vapor composition with the fractions of neutral ion pairs (NIPs) and decomposition products dependent on evaporation conditions such as the IL volume to surface ratio [1, 4] or the evaporation to effusion area ratio [2, 3, 6]. The ambiguity of the factors that determine evaporation/decomposition competition calls for new research on this topic. In our recent work [3] a new approach to analysis of the complex vapor composition was developed on the example of 1-butyl-3-methylimidazolium tetrafluoroborate ($BMImBF_4$). It includes mass spectrometric investigation of IL under different evaporation conditions: 1) in equilibrium inside an effusion cell (EC), 2) in nonequilibrium over open IL surface (OS), 3) in intermediate conditions in an open cell (OC). In this work we apply the same approach for 1-ethyl-3-methylimidazolium hexafluorophosphate ($EMImPF_6$) being a representative of alkyl-imidazolium ILs with the PF_6^- anion. This IL is expected to decompose according to reaction

$$EMImPF_{6,\,s} = C_6N_2H_{10}PF_{5,\,g} + HF,_{\,g}, \qquad \text{(I)}$$

where $C_6N_2H_{10}PF_5$ is 1-ethyl-3-methylimidazolium-2-pentafluorophosphate.

The complex vapor composition makes it difficult to determine the thermodynamic characteristics of the vaporization. Up to date the only investigation of the vaporization thermodynamics of $EMImPF_6$ is the work of Zaitsau et al. [7] performed by the quartz-crystal microbalance (QCM) method. The thermodynamic quantities in [7] were measured under nonequilibrium Langmuir conditions without any control of the gas phase composition. The goal of this work is to carry out a thorough investigation of the vapor species over $EMImPF_6$ and to determine the thermodynamic parameters of its sublimation.

2. Materials and Methods

$EMImPF_6$ is in the solid state at room temperature (T_m = 333 K [8]). IR spectra of solid samples (99% purity, Abcr GmbH, Karlsruhe, Germany) were obtained by a Bruker Tensor 27 FTIR Spectrometer in 4000-400 cm^{-1} spectral range with 1 cm^{-1} resolution.

1H, 13C, and 31P NMR spectra in DMSO-d6 at room temperature were recorded by a Bruker Avance III 500 (Bruker AXS, Madison, US) spectrometer with 5 mm TBI 1H/31P/D-BB z-GRD sensor. Detailed description of the apparatus was given elsewhere [2].

Mass spectrometric experiments were carried out in the electron ionization mode (E = 40 eV) with the use of a magnetic sector apparatus MI1201. Evaporation of the samples was performed from molybdenum Knudsen cells. Two cells with different ratios of evaporation area to effusion area, about 600 (EC-I) and about 200 (EC-II), were used. Sample heating was controlled by the temperature regulator OWEN TRM101 coupled with a tungsten-rhenium thermocouple. The melting point of lithium (453.69 K) was used to calibrate the temperature with an accuracy of ±3 K. A detailed description of the mass spectrometer is given elsewhere [9, 10, 11].

To study the decomposition products IL was evaporated during 1.5 h at T = 630 K under high vacuum and the distillate was collected and analyzed. The experiment was carried out until the sample in effusion cell was completely distilled.

Computations of the thermochemical data of the studied compounds were performed in the Gaussian 16 environment [12] using the composite G4 method [13]. A detailed description of the method is given elsewhere [14]. The thermodynamic functions (enthalpy increment $H°(T)–H°(0)$, reduced Gibbs energy $\Phi°(T)$) of the compounds in the ideal gas state were computed on a basis of the molecular parameters obtained at B3LYP/6-31G(2df,p) level of theory in rigid rotor – harmonic oscillator approximation using

StatThermo software [15]. The uncertainties in $\Phi°(T)$ were assessed as 2% according to [16].

3. Results and discussion

3.1. IR spectroscopy

The IR spectrum of the initial IL (Figure 1) is in good agreement with the literature one [17]. The spectrum of the residue after KEMS is generally close to that of the initial IL; a few minor new peaks appeared indicate presence of the traces of the decomposition products in the condensed phase. In the spectrum of the distillate these peaks become more distinct and some additional signals are appeared. The intensity of the bands related to the C-H stretching vibrations in the aromatic ring (3200 and 3050 cm^{-1}) is much lower in the distillate than in the initial sample. The intensity of the peak at 915 cm^{-1} corresponding to the out-of-plane C2-H vibration and 1250 cm^{-1} corresponding to the rocking C2-H vibration becomes weaker in the distillate. This fact points out a substitution of the hydrogen atom in the C2 position in the IL during the formation of decomposition products.

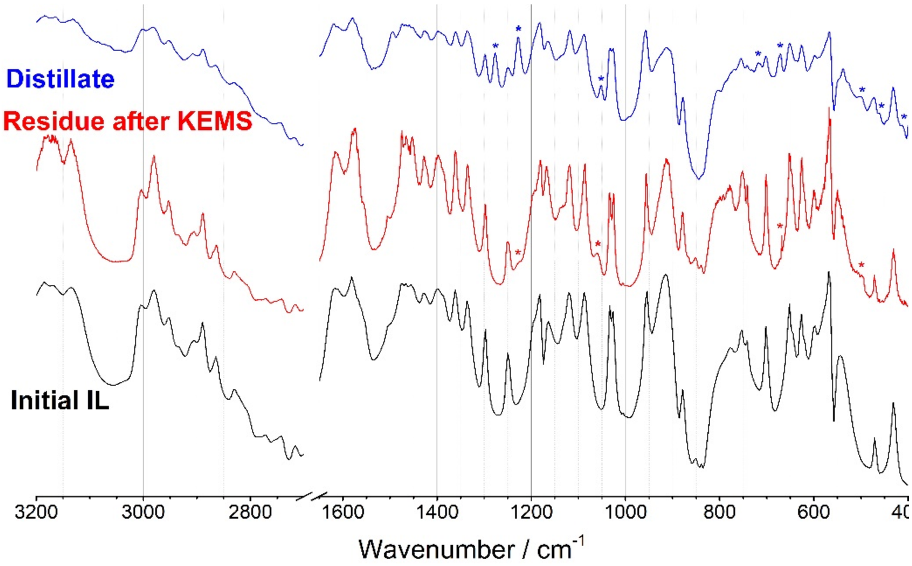

Figure 1. IR-spectra of the studied compounds. Peaks corresponding to decomposition products are marked by the asterisk

3.2. NMR-analysis

The ^{1}H NMR spectra (Figure 2) of the initial IL and the residue after KEMS are identical indicating the absence of the decomposition products in the solid phase in a significant amount. However, the spectrum of the distillate clearly differs from the previous ones showing the presence of the decomposition products. The signals of C4-H, C5-H, and C8-H protons are shifted upfield by ~0.09 ppm. A similar behavior was observed for the BMImBF$_4$ ionic liquid [4]. In contrast, the peaks of C6-H protons are shifted downfield by 0.12 ppm. A new small singlet signal at 1.24 ppm is appeared. The considerable decrease of the C2-H proton intensity is a distinctive feature of the distillate spectrum indicating the formation of 1-ethyl-3-methylimidazolium-2-pentafluorophosphate ($C_6N_2H_{10}PF_5$) by substitution of hydrogen in the C2 position. The relative amount of $C_6N_2H_{10}PF_5$ was assessed by integration of the C4-H and C5-H signals to be ~90%. None of the traces of any imidazoles were found in the distillate.

The ^{13}C and ^{31}P NMR spectra (Figure 3-4) confirmed the $C_6N_2H_{10}PF_5$ formation. In the ^{13}C spectrum the C4, C7, and C8 signals are shifted downfield by 0.4, 0.7, and 1 ppm, respectively. The maximum shift 2.0 ppm downfield is observed for the C6 atom. The C5 signal is shifted by 0.7 ppm upfield in the distillate spectrum. It should be noted that the C4 and C5 signals in the distillate spectrum are doublets, appearing due to the spin-spin interaction of these atoms with the PF_5 group in the C2 position. This phenomenon was also observed for the homologous BMImPF$_6$ IL [4]. The C2 signal is almost completely disappeared. The changes in the ^{31}P spectra are more evident. Not only shifts of the signals but also changing of the number of peaks from septet to sextet was observed. This clearly indicates the transformation of the PF_6^- anion into the PF_5 group in substituted imidazole-2-ylidene.

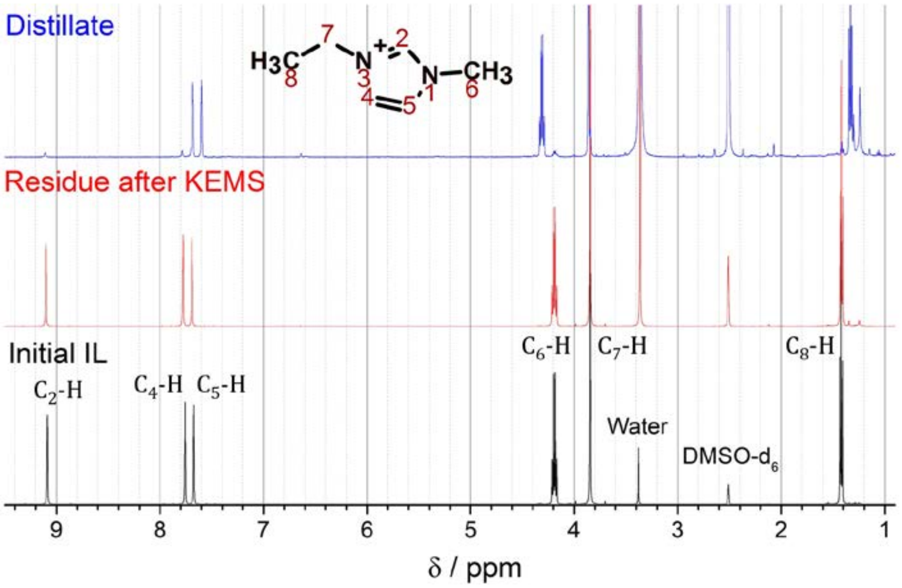

Figure 2. ^{1}H NMR spectra of studied compounds

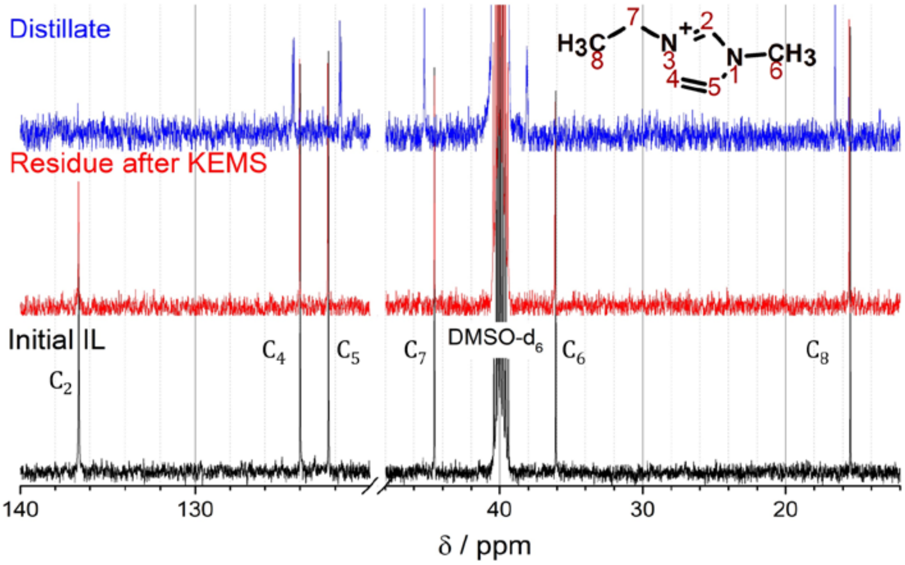

Figure 3. ^{13}C NMR spectra of studied compounds

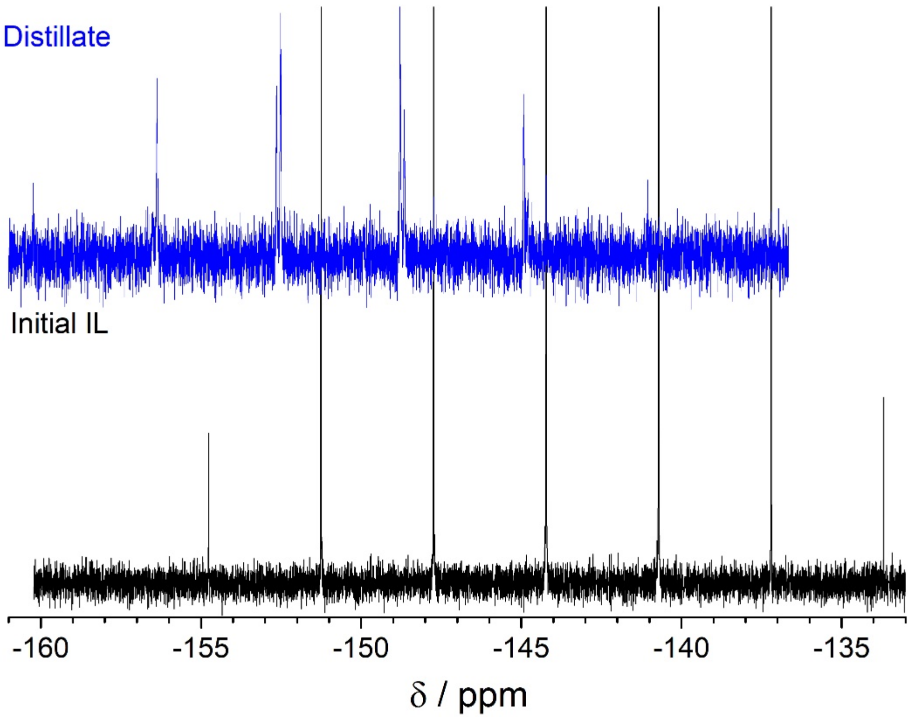

Figure 4. ^{31}P NMR spectra of studied compounds

3.3. KEMS

The background subtracted electron ionization mass spectra of the most intensive ions under different evaporation conditions are shown in Figure 5. The full-scale mass spectra of the EMImPF$_6$ can be found in Supplementary Materials (Figure S1-S4). One can see that spectra under OC conditions are temperature independent. Under equilibrium conditions, a slight temperature trend of increasing intensity of ions corresponding to the fragmentation of $C_6N_2H_{10}PF_5$ (see below) was revealed. During the analysis of the mass spectra presented in Figure 5 and Figure 6 the intensity of the parent cation $C_6N_2H_{11}^+$ was corrected by the intensity of the second isotope of the ion $C_6N_2H_{10}^+$ since the latter makes a significant contribution to the peak with *m*/*z* = 111. The ion with *m*/*z* = 82 is dominating under equilibrium conditions while under OS and OC conditions the parent cation with *m*/*z* = 111 is the most intensive. In all spectra except OS the ions corresponding to fragmentation of $C_6N_2H_{10}PF_5$ are present. The peak with *m*/*z* = 217 corresponds to fluorine detachment ($C_6N_2H_{10}PF_4^+$) and that with *m*/*z* = 169 corresponds to a cleavage of $C_6N_2H_{10}PF_4^+$ onto C_2H_5F and $C_4N_2H_5PF_3^+$. All these ions are fingerprints of the formation of the substituted imidazole-2-ylidene. Similar ions were observed in the homologous BMImPF$_6$ in our work [4].

Under OC conditions, two interesting ions appear in the spectrum. One of them with *m*/*z* = 130 corresponds to the fluorine attachment to the parent cation. The same kind of ions were previously registered in similar BMImPF$_6$ and BMImBF$_4$ ILs [2, 3, 4, 18]. The scheme of the formation of this ion is given in [18]. Another ion with *m*/*z* = 367 registered at 524 K (0.2% of the parent cation intensity) corresponds to the formula C_2A^+, where C is the parent cation and A is the PF_6^- anion. This fact indicates the formation of a small amount of NIP dimer. Previously, dimerization was observed only for the ILs evaporated without decomposition [19].

The mass spectrum recorded under OS conditions contains only ions with *m*/*z* = 82, 110, 111. As it is shown earlier [2], evaporation in nonequilibrium condition suppresses the decomposition processes and the OS spectrum corresponds to that of NIP.

The mass spectrum of the distillate (Figure 6) corresponding to that of $C_6N_2H_{10}PF_5$ contains the following major ions (relative to intensity of ion with $m/z = 82$): 82 (100%), 217 (60%), 110 (50%), 169 (17%), 107 (15%), 81 (12%). The full-scale mass spectrum of the distillate is given in Supplementary Materials (Figure S5).

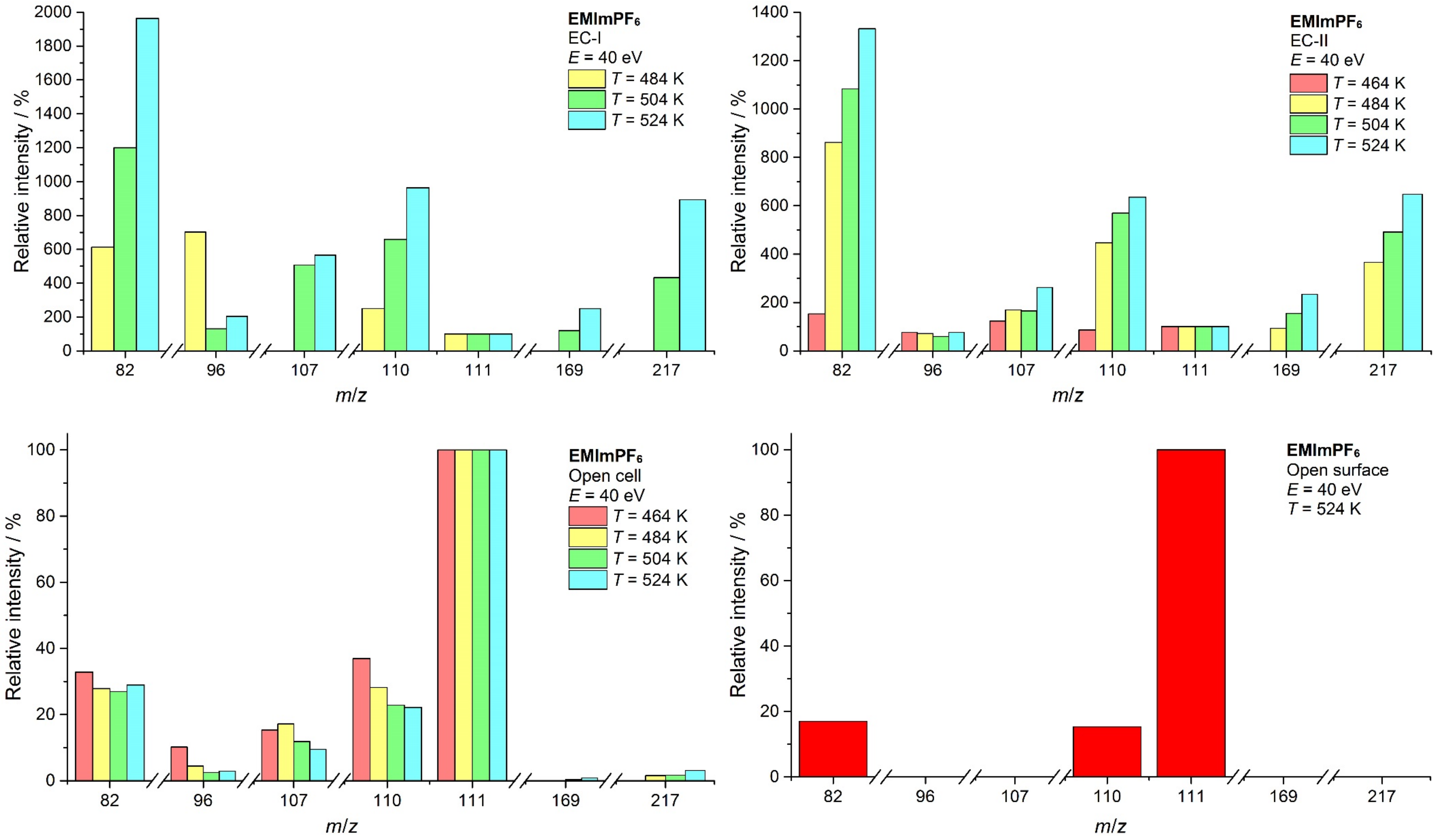

Figure 5. Mass spectra of EMImPF$_6$ under different conditions (intensity of the peak with *m*/*z* = 111 was taken as 100%)

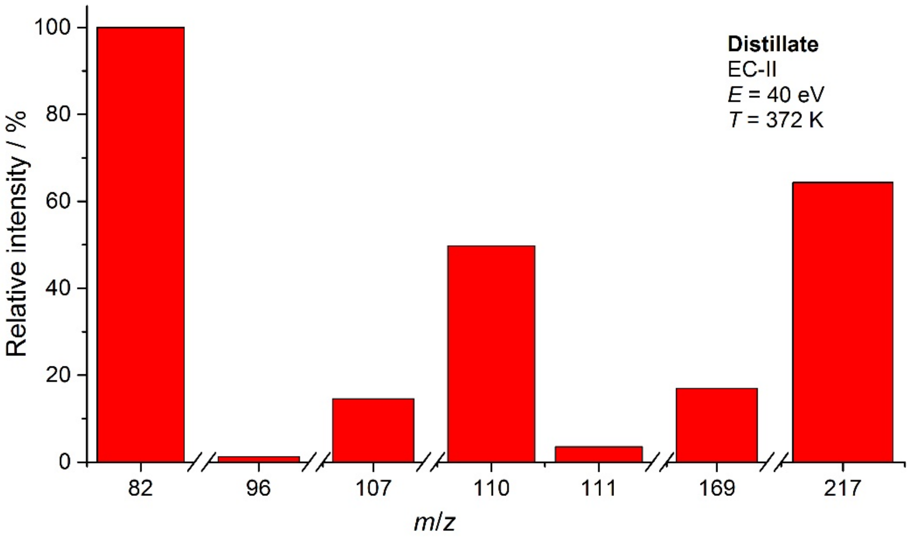

Figure 6. Mass spectrum of distillate at T = 382 K and E = 40 eV (intensity of the peak with m/z = 82 was taken as 100%)

Ionization efficiency curves (IEC) for the most intensive ions were measured under different conditions and temperatures (Figure 7). The energy scale was calibrated by the ionization energy of H_2O (IE = 12.62 eV [20]). Appearance energies (AE) of the ions were determined by the vanishing current method (Table 1).

The AE values of the ions with m/z = 82 and 110 under both EC-I and EC-II conditions are temperature independent. Comparison of their AEs between EC and OC reveals a slight decreasing tendency against temperature. Both of these ions are also present in the OS mass spectrum and can originate from NIPs; the low intensity of the ion currents did not allow measuring their IECs under OS conditions. The values AE(82) = 9.9±0.3 eV and AE(110) = 8.6±0.1 eV being the average among EC-I, EC-II, OC (464 K), and OC (484 K) decrease by 2.0 and 0.6 eV, respectively under OC (524 K) conditions. This behavior can be explained as follows. Under equilibrium conditions, the major contribution into the current of these ions is due to decomposition products. The transition from the Knudsen conditions to the Langmuir conditions is accompanied by a decrease in the amount of decomposition products, therefore the contribution from NIPs becomes greater leading to decreasing of the AE values. The AE values of the ions with m/z = 130 and 367 under OC conditions at 524 K are 10.3±0.5 eV and 10.9±0.5 eV, respectively.

IECs for the IL distillate measured under EC-II conditions at 374 K are shown in Supplementary Materials (Figure S6). AEs of the main ions are collected in Table 1. One can see that they are close to those obtained on equilibrium conditions, confirming our suggestion that the $C_6N_2H_{10}PF_5$ is the main molecular precursor of the ions with m/z = 82 and 110. The AE(217) = 13.7±0.5 eV for distillate agrees with that measured for IL under EC-II conditions at 484 K (13.1±0.5 eV).

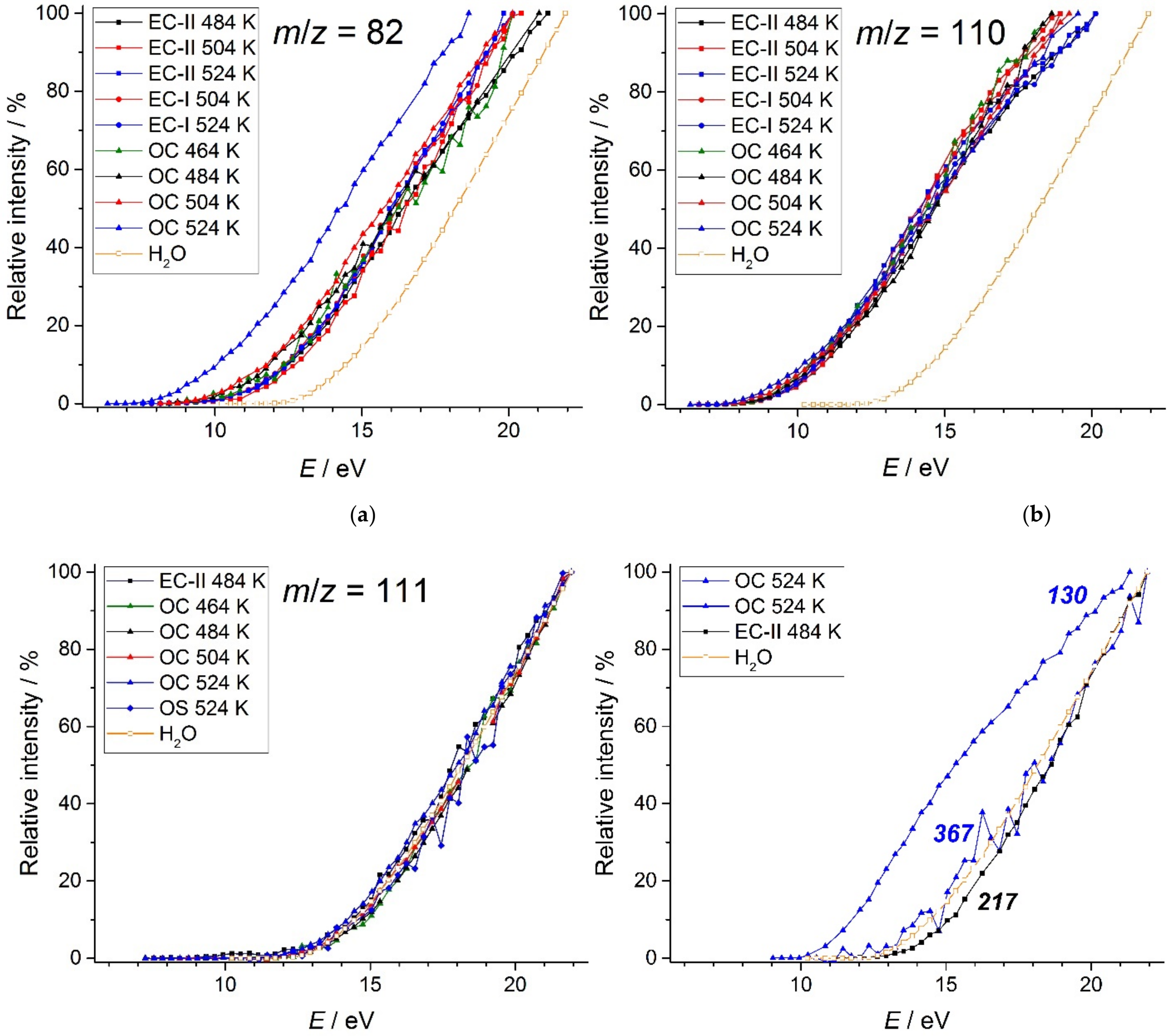

(a) (b)

(c) (d)

Figure 7. Ionization efficiency curves of ions with *m*/*z* = 82 (**a**), 110 (**b**), 111 (**c**), and others (**d**) in mass spectra of EMImPF$_6$ under different evaporation conditions

The temperature dependencies of the ion currents were measured under different evaporation conditions and their slope tangents are collected in Table 2. One can see that the slope of the temperature dependence of the ion with *m*/*z* = 111 is near under all conditions. The slopes for ions with *m*/*z* = 110, 111, and 130 under OC and EC-II conditions are very close to each other indicating NIPs as the common source of their origination. The slope for an ion with *m*/*z* = 217 corresponding to the detachment of fluorine from $C_6N_2H_{10}PF_5$ is rather high (-16.4). As expected, the ions with *m*/*z* = 82 and 110 have two sources of origination: NIPs and $C_6N_2H_{10}PF_5$. Hence, their slopes are intermediate values as it is shown in Table 2.

Table 1. Appearance energies (*AE*, ±0.5 eV) of main ions at different evaporation conditions

Conditions	***T* / K**	***m/z***		
		82	**110**	**111**
		IL		
EC-I	504	10.0	8.5	
	524	10.0	8.5	
EC-II	484	9.8	8.8	12.1
	504	10.2	8.8	
	524	10.1	8.6	
OC	464	9.5	8.6	12.4
	484	9.5	8.6	12.4
	504	9.4	8.3	12.3
	524	7.9	8.0	12.0
OS	524			11.9
		Distillate		
EC-II	374	11.4	9.6	

To identify the molecular precursors of the observed ions, the dependencies of the relative ion currents on the evaporation conditions are studied (Figure 8). One can see that the difference between the EC-I and EC-II conditions is negligible. The absence of a trend of the 130/111 ratio confirmed the suggestion that NIP is their common source. The same situation occurs for the 169/217 ratio pointing out the formation of both these ions from $C_6N_2H_{10}PF_5$. An ion with *m/z* = 110 under equilibrium conditions is primarily formed from substituted imidazole-2-ylidene, while under nonequilibrium conditions NIP is its main source. The main change in the considered ratios is observed at the transition from equilibrium (EC-I and EC-II) to nonequilibrium and intermediate (OC and OS) conditions. One can see that the ratios 82/111 and 110/111 are very close for OC and OS conditions indicating that in OC conditions the intensities of these ions are primarily determined by the contribution from NIPs.

Table 2. Slope tangents of temperature dependence of ion currents at different evaporation conditions

Conditions	**EC-I**	**EC-II**	**OC**
Δ*T* / K	474-511	463-523	454-525
m/z			
82	-16.457±0.763	-17.349±0.498	-15.240±0.379
110	-15.636±0.544	-14.732±0.375	-14.702±0.232
111	-14.049±0.227	-14.910±0.209	-14.634±0.245
130			-14.242±0.234
217	-16.839±1.097	-16.248±0.943	

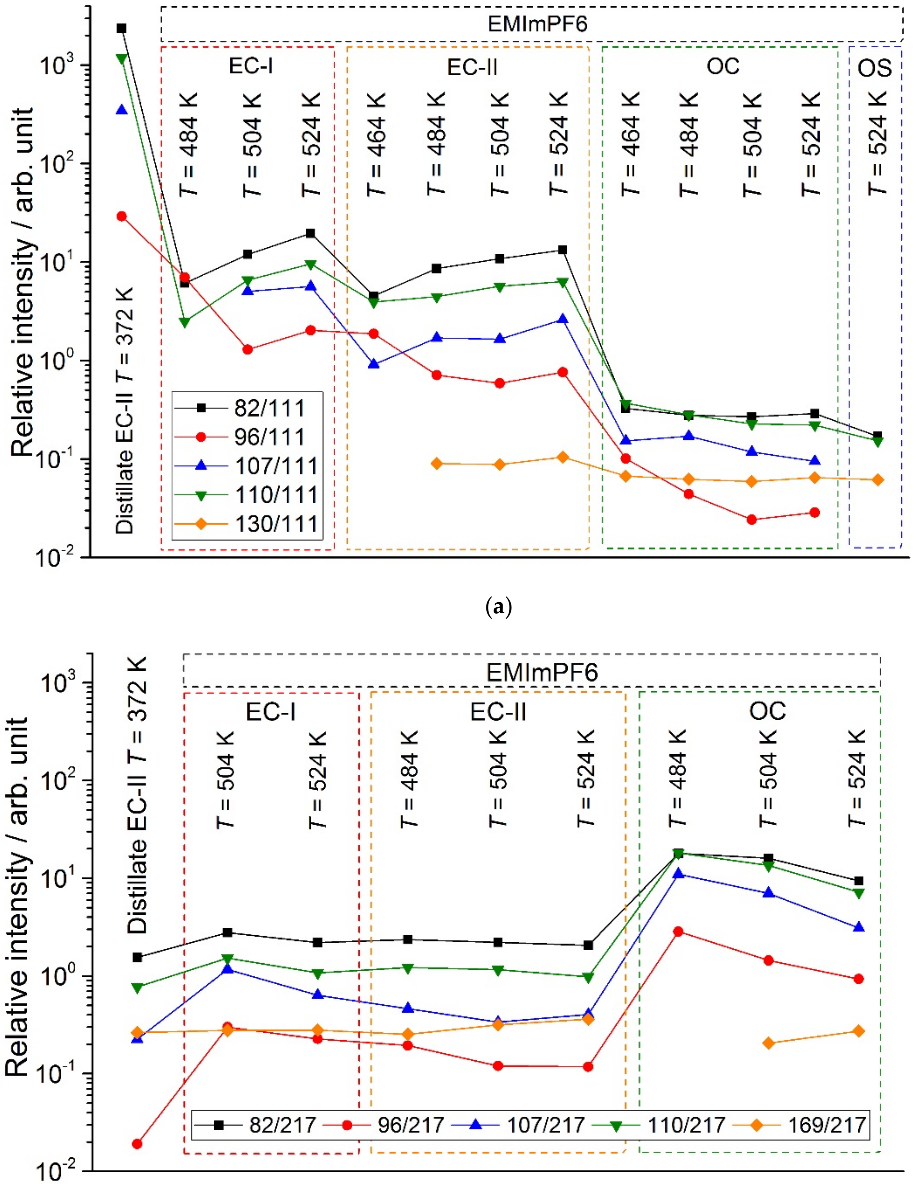

(**a**)

(**b**)

Figure 8. Dependence of relative intensity of ion currents on evaporation conditions: (**a**) – relative to *m*/*z* = 111; (**b**) – relative to *m*/*z* = 217

Based on the above conclusions the following scheme of fragmentation of the vapor species is suggested (Figure 9). Some ions having only one molecular precursor are fingerprints of NIPs (*m*/*z* = 111 and 130) and $C_6N_2H_{10}PF_5$ (*m*/*z* = 169 and 217), while the others have two precursors.

The quantitative interpretation of the mass spectra was performed on a basis of the fragmentation coefficients derived from the OS mass spectrum of IL (NIP is the only molecular precursor) and the spectrum of the distillate ($C_6N_2H_{10}PF_5$ is the only molecular precursor). The contributions into the ion intensities from different sources were found by the following equations:

$$I(82/\mathrm{NIPs}) = k(82/\mathrm{NIPs})\cdot I(111), \tag{1}$$

$$I(110/\mathrm{NIPs}) = k(110/\mathrm{NIPs})\cdot I(111), \tag{2}$$

$$I(130/\mathrm{NIPs}) = k(130/\mathrm{NIPs})\cdot I(111), \tag{3}$$

$$I(82/C_6N_2H_{10}PF_5) = k(82/C_6N_2H_{10}PF_5)\cdot I(217), \quad (4)$$
$$I(96/C_6N_2H_{10}PF_5) = k(96/C_6N_2H_{10}PF_5)\cdot I(217), \quad (5)$$
$$I(107/C_6N_2H_{10}PF_5) = k(107/C_6N_2H_{10}PF_5)\cdot I(217), \quad (6)$$
$$I(110/C_6N_2H_{10}PF_5) = k(110/C_6N_2H_{10}PF_5)\cdot I(217). \quad (7)$$

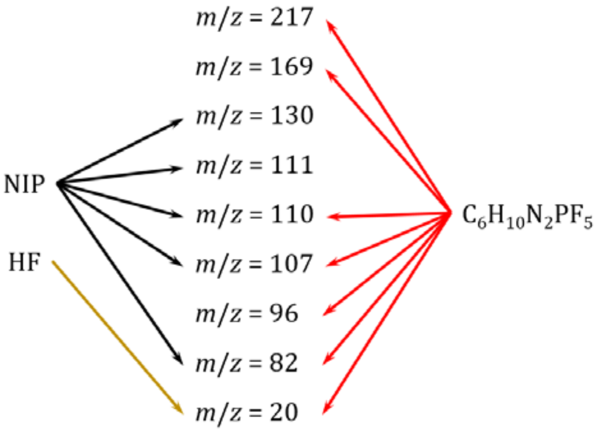

Figure 9. Scheme of fragmentation of the vapor species of EMImPF$_6$

The fractions of the vapor components (Figure 10) were calculated. One can see from Figure 8 that the vapor composition is almost temperature independent. Under equilibrium conditions, the substituted imidazole-2-ylidene $C_6N_2H_{10}PF_5$ dominates. The transition to Langmuir conditions leads to a significant increase of the NIP fraction in vapor.

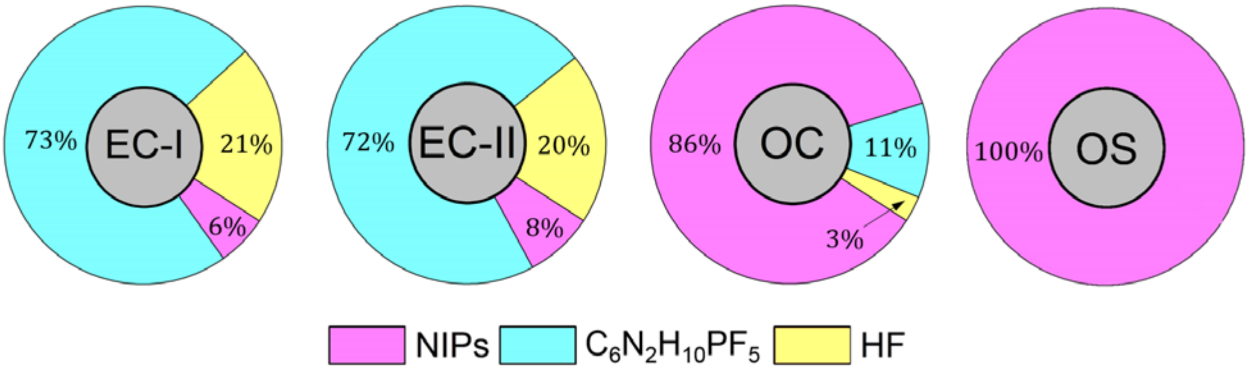

Figure 10. Fractions of the vapor components under different evaporation conditions

The value of thermodynamic activity of IL is an important question to perform thermodynamic calculations of sublimation enthalpy. Decomposition products are high volatile and do not accumulate in the condensed phase as shown by NMR and IR spectroscopy of the IL residue after KEMS (see above). Hence the IL composition is practically unchanged and its activity is close to unity.

The partial pressures of the vapor species in the Knudsen cell were obtained using their fractions (Figure 10) and the total vapor pressure found by the Knudsen effusion method. The procedure was described earlier [21] The experiment was carried out at T = 540 K during 19 h using EC-I. The effective area of the effusion orifice, $s = (3.40\pm0.66)\cdot10^{-8}$ m^2, was determined by sublimation of pure zinc, see [21] for details. The average molar

Preprints (www.preprints.org) | NOT PEER-REVIEWED | Posted: 5 May 2023 doi:10.20944/preprints202305.0349.v1

mass of the EMImPF$_6$ IL vapor, M = 191.9 kg·kmol^{-1}, was calculated from the molar masses of the effusion products and their fractions (Figure 10). The found total vapor pressure (0.67 Pa) was used to obtain the sensitivity constant of the mass spectrometer. The experimentally measured ion currents were recalculated into the partial vapor pressures (Table 3) according to a conventional mass spectrometric procedure described elsewhere in details [19]. The temperature dependencies of the vapor pressures (Figure 11) in the form ln(p) = f(1000/T) were approximated by a linear equation ln(p/Pa) = a·10^3/T + b with the a and b coefficients given in Table 4. One can see from Figure 11 that the vapor pressure of NIPs obtained in this work is close to that from [7].

Table 3. Partial pressures (·10^4 Pa) of vapor species over EMImPF$_6$ under EC conditions

T / K	**NIPs**	**$C_6N_2H_{10}PF_5$**	**HF**
524	16.0	157	45.6
514	10.3	117	34.0
505	6.60	79.0	23.0
494	3.51	30.9	8.99
484	1.73	16.1	4.70
474	0.93	6.93	2.02
464	0.37	4.84	1.41
469	0.63	3.92	1.14
479	1.30	8.01	2.33
488	2.51	17.3	5.04
499	4.44	41.6	12.1

Table 4. Coefficients of the equation ln(p/Pa) = a·10^3/T + b

Vapor species	***a***	***b***
	Ionic liquid (464-524 K)	
NIPs	-14.977±0.380	24.592±0.776
$C_6N_2H_{10}PF_5$	-16.184±0.867	29.239±1.772
HF	-16.184±0.867	28.005±1.772
	Distillate (332-374 K)	
$C_6N_2H_{10}PF_5$	-10.384±0.166	25.892±0.475

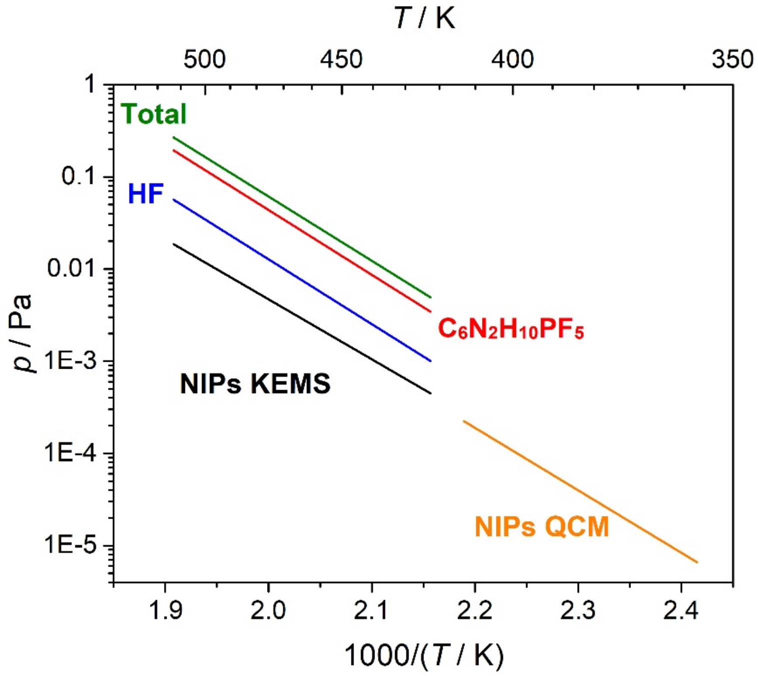

Figure 11. Temperature dependencies of pressure of the vapor species over EMImPF$_6$. NIPs QCM data are taken from [7]

The thermodynamic functions of the EMImPF$_6$ IL in the condensed state needed for thermochemical calculations were obtained from the temperature dependencies of the molar heat capacity. The available literature data [22, 23, 24] on heat capacity are restricted to $T = 355$ K and have only four points above melting. Since heat capacity of liquids usually poorly depends on temperature, the $c_p°$ values above experimental temperatures were taken as a constant equal to $c_p°(355\ \text{K}) = 374\ \text{J·mol}^{-1}\text{·K}^{-1}$. $S°(\text{EMImPF}_{6,\text{cr}}, 298.15\ \text{K}) = 353\ \text{J·mol}^{-1}\text{·K}^{-1}$ was assessed by the method proposed by Glasser and Jenkins [25]. The density of EMImPF$_6$ in the condensed state needed for the entropy assessment was taken from [26]. The thermodynamic functions $H°(T)–H°(298.15)$ found in this way are in good agreement with those obtained by an alternative method given in [7] based on the thermal expansion coefficient, isothermal compressibility, and molar volume. The thermodynamic functions used in this work were approximated by polynomial

$$\Phi'°(T) = \frac{G°(T)-[H°(T)-H°(298.15\ \text{K})]}{T} = a\ln x + bx^{-2} + cx^{-1} + dx + ex^2 + fx^3,\ (x = T/1000), \qquad (8)$$

the coefficients of which are given in Table 5.

Table 5. Coefficients of polynomial (8)

Compound	ΔT / K	a	b, $\cdot 10^{-3}$	c	d, $\cdot 10^3$	e, $\cdot 10^4$	f, $\cdot 10^4$
EMImPF$_{6,\text{ s}}$	298.15-334	1998	-1035	170.5	154.2	-240.3	1340
EMImPF$_{6,\text{ s}}$	334-600	9.847	-8.787	5.077	8.156	-2.304	-5.235
EMImPF$_{6,\text{ g}}$	298.15-600	-74.95	7.229	2.427	7.009	-2.240	4.391
$C_6N_2H_{10}PF_{5,\text{ g}}$	298.15-600	-63.76	5.581	2.336	6.232	-1.911	3.562

The sublimation enthalpies (Table 6) found in this work by the methods of the second and third law (see Table S2) agree to each other and to the values from [7] as well. Taking into account large uncertainties of the thermodynamic functions, the second law data are preferable. The value $\Delta_s H°(298.15\ \text{K}) = 157 \pm 6\ \text{kJ·mol}^{-1}$ being an average between our data and those from [7] was recommended. Using this value and $\Delta_f H°(\text{EMImPF}_{6,\text{ s}}, 298.15\ \text{K}) =$

–2098.9±4.7 kJ·mol^{-1} measured by solution calorimetry [7], the formation enthalpy of EMImPF$_6$ NIPs was found as –1942±8 kJ·mol^{-1}.

$\Delta_f H°$(EMImPF$_{6,\ g}$, 298.15 K) was also calculated by the isodesmic reaction approach with the use of the composite G4 method. The required experimental data on the formation enthalpies of the reactants are taken from [27, 28]. A full list of reactions used as well as the obtained formation enthalpies can be found in Supplementary Materials (Table S1). All values were treated by the Student's method and the average $\Delta_f H°$(EMImPF$_{6,\ g}$, 298.15 K) = –1937±3 kJ·mol^{-1} was evaluated. This enthalpy is in good agreement with the experimental one.

Table 6. Reaction enthalpies $\Delta_r H°$ (kJ·mol^{-1}) and entropies $\Delta_r S°$ (J·mol^{-1}·K^{-1}), temperature range ΔT (K), mean harmonic temperature T (K), number of measurements N

ΔT	T	N	$\Delta_r H°(T)$	$\Delta_r H°$(298.15 K)		$\Delta_r S°(T)$		Method[3]	Conditions	Ref.
				II law[1]	III law[2]	II law[1]	III law[2]			
				EMImPF$_{6,\ s,l}$ = EMImPF$_{6,\ g}$						
464-524	490	11	125±3	156±4	152±14	109±4	102±18	KEMS	EC-II	this work
414-457	436	18	130±1	158±2	153±14	118±1	108±18	QCM	OS	[7]
				EMImPF$_{6,\ g}$ = $C_6N_2H_{10}PF_{5,\ g}$ + HF$_{,\ g}$						
464-524	490	11	145±8	144±9	112±14	176±24	110±18	KEMS	EC-II	this work

[1] The standard deviations are given for $\Delta_r H°(T)$. When $\Delta_r H°(T)$ were recalculated to 298.15 K their uncertainties were increased by those in thermodynamic functions estimated as 2% from $H°(T)$–$H°$(298.15) of NIP [16];

[2] Uncertainty is mainly determined by that in thermodynamic functions estimated as 2% from $\Phi'(T)$ of NIP [16] and 6% from $S°(T)$ of IL [25];

[3] Methods: Knudsen effusion mass spectrometry (KEMS) and quartz micro balance (QCM).

The enthalpy of the gas-phase reaction (I) was calculated using experimentally determined partial pressures by the method of the second and third law (Table 6 and Fig S7). One can see large discrepancies in the obtained enthalpies and entropies. Theoretical calculation of the reaction enthalpy using G4 method gives $\Delta_r H°$(298.15 K) = 75 kJ·mol^{-1}, which is much below both experimental values. It means that the experimental partial pressures of the decomposition products do not reach their equilibrium values. This phenomenon can be explained as the partial equilibrium caused by the kinetically hindered decomposition. Such behavior was previously observed for the similar BMImPF$_6$ IL [3, 4].

To test the kinetic factor influence, the time dependencies of the intensity of the ions with m/z = 111 (corresponding to NIPs) and m/z = 110 (corresponding to $C_6N_2H_{10}PF_5$) were measured at cooling and heating between 484 and 504 K under EC-II conditions with 20 s step (heating rate is 5 K/min). The relative gain/loss of intensity were calculated according to following formula:

$$\Delta I_i = \frac{|I_i - I_0|}{I_{max}} * 100\%, \qquad (9)$$

where I_0 is the ion current at the starting temperature, I_{max} the maximal ion current.

ΔI of an ion with m/z = 111 rises and falls faster than that with m/z = 110 (Figure 12). A rate of the intensity changes was found as a first derivative of the time dependence of the relative ion current. The rate of reaching a steady-state for an ion with m/z = 111 is higher than that with m/z = 110 both at heating and cooling. This fact indicates that the attainment of equilibrium in decomposition reaction (I) is kinetically hindered and any thermodynamic calculations for the decomposition products ($C_6N_2H_{10}PF_{5,\ g}$ and HF$_{,\ g}$) are impossible.

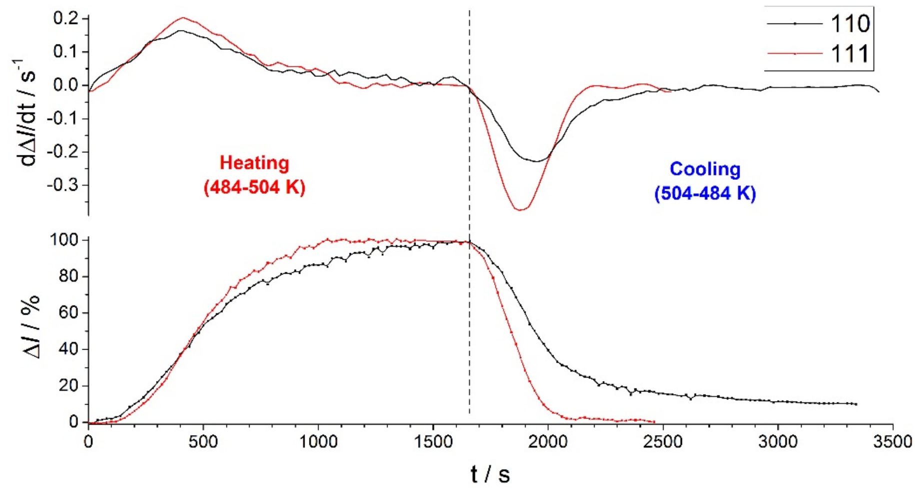

Figure 12. Time dependence of the relative gain/loss of intensity of ions with *m*/*z* = 111 and 110 (down) and its first derivative (up)

The temperature dependencies of the ion currents measured for the IL distillate (90% of $C_6N_2H_{10}PF_5$, Figure S8) show that in the temperature range 332-374 K all ions are characterized by the close slopes indicating a single source of their origination. The determined vapor pressure of $C_6N_2H_{10}PF_5$ was fitted by a linear equation with coefficients given in Table 4. The plot of the temperature dependence of the vapor pressure is given in Supplementary materials (Figure S9). The assessed activity $a(C_6N_2H_{10}PF_5) \leq 2\cdot10^{-4}$ at an average temperature of the KEMS study of $EMImPF_6$ confirms our assumption that the activity of IL is close to 1. The upper limit of the assessed $C_6N_2H_{10}PF_5$ activity is determined by the fact that the studied distillate is not pure substituted imidazole-2-yidene. The sublimation enthalpy and entropy of $C_6N_2H_{10}PF_5$ at $T = 350$ K were 86±1 $kJ\cdot mol^{-1}$ and 120±4 $J\cdot mol^{-1}\cdot K^{-1}$, respectively. The value of sublimation enthalpy is close to those of substituted alkylimidazoles [29]. The enthalpy of the $C_6N_2H_{10}PF_{5,\,g}$ formation at 298.15 K (–1594±6 $kJ\cdot mol^{-1}$) was calculated from the theoretical enthalpy of the reaction II and the found value $\Delta_f H°(EMImPF_{6,\,g}$, 298.15 K).

5. Conclusions

Heating of $EMImPF_6$ IL is accompanied by competing vaporization and decomposition processes. The evaporation to effusion ratio is a key factor determining the relationship between them. It was established that under Langmuir conditions the vapor over IL consists of NIPs only, whereas under equilibrium conditions in the temperature range (464 – 524 K) the decomposition products are dominating. The latter are highly volatile and do not accumulate in the significant amount in the condensed phase. To identify their nature the IL distillate was collected and analyzed. The analysis provided by the IR and NMR spectroscopy reveals that the IL distillate is 1-ethyl-3-methylimidazolium-2-pentafluorophosphate ($C_6N_2H_{10}PF_5$). No traces of any imidazoles were found. Therefore, there is only one decomposition path – onto $C_6N_2H_{10}PF_5$ and HF. The vapor pressure of $C_6N_2H_{10}PF_5$ obtained by KEMS is used to assess a value of thermodynamic activity ($<10^{-4}$) of the decomposition products in IL. It was assumed that the vapor pressures of the decomposition products do not attain the equilibrium ones and thus the decomposition process is kinetically hindered. This assumption was supported by the measurements of the time dependencies of the ion currents corresponding to NIPs and $C_6N_2H_{10}PF_5$ on the one hand, and by the calculation of the enthalpy of the gas-phase decomposition reaction on the other hand.

The NIP vapor pressure and the sublimation enthalpy of EMImPF$_6$ found in this work (156±4 kJ·mol^{-1} at 298.15 K) are in agreement with the corresponding literature data [7] found in Langmuir conditions. This fact indicates that the vaporization coefficient of EMImPF$_6$ in the form of NIPs is close to unity; the same conclusion was done earlier for the similar BMImBF$_4$ IL [3]. Taking into account the melting enthalpy 17.7 kJ·mol^{-1} [23] for the EMImPF$_6$ IL, its sublimation enthalpy is reasonably consistent to the vaporization enthalpy of the thermally stable EMImNTf$_2$ IL ($\Delta_vH°$(298.15 K) = 135.3±1.3 kJ·mol^{-1} [30]). The combination of the experimental formation enthalpy of solid EMImPF$_6$ and the obtained sublimation enthalpy gives $\Delta_fH°$(EMImPF$_{6,\ g}$, 298.15 K) = –1942±8 kJ·mol^{-1} being in good agreement with that calculated using the composite G4 method.

Author Contributions: Conceptualization, A.D.; methodology, V.M.; software, D.G., V.A.; validation, L.K.; formal analysis, A.D., V.M., M.K.; investigation, V.M., V.A., M.K.; resources, D.G.; writing—original draft preparation, A.D.; writing—review and editing, V.M.; visualization, A.D.; supervision, L.K.; project administration, A.D.; funding acquisition, A.D. All authors have read and agreed to the published version of the manuscript.

Funding: This research was funded by Russian Science Foundation under grant № 21-73-00041. The study was carried out using the resources of the Center for Shared Use of Scientific Equipment of the ISUCT (with the support of the Ministry of Science and Higher Education of Russia, grant No. 075-15-2021-671).

Data Availability Statement: Data supporting this study are openly available from the Manuscript and Supplementary Materials.

Acknowledgments: In this section, you can acknowledge any support given which is not covered by the author contribution or funding sections. This may include administrative and technical support, or donations in kind (e.g., materials used for experiments).

Conflicts of Interest: The authors declare no conflict of interest.

References

1. Taylor, A.W.; Lovelock, K.R.J.; Jones, R.G.; Licence, P. Borane-substituted imidazol-2-ylidenes: syntheses in vacuo. *Dalton Trans.* **2011**, *40*, 1463–1470. DOI: 10.1039/C0DT01240H
2. Dunaev, A.M.; Motalov, V.B.; Kudin, L.S. The Composition of Saturated Vapor Over 1-Butyl-3-Methylimidazolium Tetrafluoroborate Ionic Liquid: A Multi-Technique Study of the Vaporization Process. *Entropy* **2021**, *23*, 1478. DOI: 10.3390/e23111478
3. Dunaev, A.M.; Motalov, V.B.; Kudin, L.S.; Zhabanov, Yu.A.; Aleksandriiskii, V.V.; Govorov, D.N. Evaporation Thermodynamics of 1-Butyl-3-methylimidazolium Tetrafluoroborate Ionic Liquid. *J. Mol. Liq.* **2023**, *380*, 121626. DOI: 10.1016/j.molliq.2023.121626
4. Clarke, C.J.; Puttick, S.; Sanderson, T.J.; Taylor, A.W.; Bourne, R.A.; Lovelock, K.R.J.; Licence, P. Thermal stability of dialkylimidazolium tetrafluoroborate and hexafluorophosphate ionic liquids: ex situ bulk heating to complement in situ mass spectrometry. *Phys. Chem. Chem. Phys.* **2018**, *20*, 16786-16800. DOI: 10.1039/c8cp01090k
5. Chambreau, S.D.; Schenk, A.C.; Sheppard, A.J.; Yandek, G.R.; Vaghjiani, G.L.; Maciejewski, J.; Koh, C.J.; Golan, A.; Leone, S.R. Thermal Decomposition Mechanisms of Alkylimidazolium Ionic Liquids with Cyano-Functionalized Anions. *J. Phys. Chem. A.* **2014**, *118*, 11119–11132. DOI: 10.1021/jp5095855
6. Volpe, V.; Brunetti, B.; Gigli, G.; Lapi, A.; Vecchio Ciprioti, S.; Ciccioli, A. Toward the Elucidation of the Competing Role of Evaporation and Thermal Decomposition in Ionic Liquids: A Multitechnique Study of the Vaporization Behavior of 1-Butyl-3-methylimidazolium Hexafluorophosphate under Effusion Conditions. *J. Phys. Chem. B*. **2017**, *121*, 10382–10393.
7. Zaitsau, D.H.; Yermalayeu, A.V.; Emel'yanenko, V.N.; Butler, S.; Schubert, T.; and Verevkin, S.P. Thermodynamics of Imidazolium-Based Ionic Liquids Containing PF$_6$ Anions *J. Phys. Chem. B*. **2016**, *120*, 7949–7957. DOI: 10.1021/acs.jpcb.6b06081
8. Vila, J.; Fernandez-Castro, B.; Rilo, E.; Carrete, J.; Dominguez-Perez, M.; Rodriguez, J. R.; Garcia, M.; Varela, L. M.; Cabeza, O. Liquid-solid-liquid phase transition hysteresis loops in the ionic conductivity of ten imidazolium-based ionic liquids *Fluid Phase Equilib*. **2012**, *320*, 1-10. DOI: 10.1016/j.fluid.2012.02.006
9. Dunaev, A.M; Kryuchkov, A.S.; Kudin, L.S.; Butman, M.F. Automatic complex for high temperature investigation on basis of mass spectrometer MI1201 *Izv. Vyssh. Uchebn. Zaved. Khim. Khim. Tekhnol*. **2011**, *54(8)*. P. 73-77. (in Russian)
10. Sergeev, D.N.; Dunaev, A.M.; Ivanov, D.A.; Golovkina, Y.A.; Gusev, G.I. Automatization of mass spectrometer for the obtaining of ionization efficiency functions *Pribory i Tekhnika Eksperimenta*. **2014**, *1*. 139-140 (in Russian), DOI: 10.7868/S0032816214010200.

11. Dunaev, A.M.; Motalov, V.B.; Kudin, L.S. A high-temperature mass-spectrometric method for determination of the electron work function of ionic crystals: Lanthanum, cerium, and praseodymium triiodides. *Russ. J. Gen. Chem.* **2017**, *87*, 632-638, DOI: 10.1134/S1070363217030410.
12. Gaussian 16, Revision C.01, Frisch, M. J.; Trucks, G. W.; Schlegel, H. B.; Scuseria, G. E.; Robb, M. A.; Cheeseman, J. R.; Scalmani, G.; Barone, V.; Petersson, G. A.; Nakatsuji, H.; Li, X.; Caricato, M.; Marenich, A. V.; Bloino, J.; Janesko, B. G.; Gomperts, R.; Mennucci, B.; Hratchian, H. P.; Ortiz, J. V.; Izmaylov, A. F.; Sonnenberg, J. L.; Williams-Young, D.; Ding, F.; Lipparini, F.; Egidi, F.; Goings, J.; Peng, B.; Petrone, A.; Henderson, T.; Ranasinghe, D.; Zakrzewski, V. G.; Gao, J.; Rega, N.; Zheng, G.; Liang, W.; Hada, M.; Ehara, M.; Toyota, K.; Fukuda, R.; Hasegawa, J.; Ishida, M.; Nakajima, T.; Honda, Y.; Kitao, O.; Nakai, H.; Vreven, T.; Throssell, K.; Montgomery, J. A., Jr.; Peralta, J. E.; Ogliaro, F.; Bearpark, M. J.; Heyd, J. J.; Brothers, E. N.; Kudin, K. N.; Staroverov, V. N.; Keith, T. A.; Kobayashi, R.; Normand, J.; Raghavachari, K.; Rendell, A. P.; Burant, J. C.; Iyengar, S. S.; Tomasi, J.; Cossi, M.; Millam, J. M.; Klene, M.; Adamo, C.; Cammi, R.; Ochterski, J. W.; Martin, R. L.; Morokuma, K.; Farkas, O.; Foresman, J. B.; Fox, D. J. Gaussian, Inc., Wallingford CT, 2016.
13. Curtiss, L. A.; Redfern, P. C.; and Raghavachari, K. Gaussian-4 theory. *J. Chem. Phys.* **2007**, *126*, 084108. DOI: 10.1063/1.2436888
14. Govorov, D. N.; Dunaev, A. M.; Motalov, V. B.; Kudin, L. S. Quantum chemical calculations of formation enthalpies of cations and anions of ionic liquids *J. Mol. Liq.* **2022**, *364*, 119996. DOI: 10.1016/j.molliq.2022.119996.
15. Dunaev, A.M.; Kudin, L.S. Statthermo® – new software for calculation of thermodynamic functions *Izv. Vyssh. Uchebn. Zaved. Khim. Khim. Tekhnol*. **2017**, *60*, 40-46. DOI: 10.6060/tcct.2017604.5490
16. Chao, J.; Hall, K.R.; Marsh, K.N.; Wilhoit, R.C. Thermodynamic properties of key organic oxygen compounds in the carbon range C1 to C4. Part 2. Ideal gas properties *J. Phys. Chem. Ref. Data*. **1986**, *15*, 1369−1436. DOI: 10.1063/1.555769
17. Katsyuba, S.A.; Zvereva, E.E.; Vidiš, A.; Dyson, P.J. Application of Density Functional Theory and Vibrational Spectroscopy Toward the Rational Design of Ionic Liquids *J. Phys. Chem. A.* **2007**, *111*, 352-370. DOI: 10.1021/jp064610i
18. Deyko, A.; Lovelock, K.R.J.; Licence, P.; Jones, R.G. The vapour of imidazolium-based ionic liquids: a mass spectrometry study. *Phys. Chem. Chem. Phys*. **2011**, *13*, 16841–16850. DOI: 10.1039/C1CP21821B
19. Dunaev, A.M.; Motalov, V.B.; Govorov, D.N.; Kudin, L.S. Dimer neutral ion pairs and associative ions in saturated vapor of 1-ethyl-3-methylimidazolium trifluoromethanesulfonate ionic liquid *Calphad* **2019**, *65*, 127–131. DOI: 10.1016/j.calphad.2019.02.011
20. "Ion Energetics Data" by Sharon G. Lias, John E. Bartmess, Joel F. Liebman, John L. Holmes, Rhoda D. Levin, and W. Gary Mallardin NIST Chemistry WebBook, NIST Standard Reference Database Number 69, Eds. P.J. Linstrom and W.G. Mallard, National Institute of Standards and Technology, Gaithersburg MD, 20899, DOI:10.18434/T4D303, (retrieved May 1, 2022).
21. Motalov, V.B.; Korobov, M.A.; Dunaev, A.M.; Dunaeva, V.V.; Kudin, L.S. Vapor pressure and thermodynamics of L-tryptophan sublimation *Russ. J. Gen. Chem*. **2021**, *91*, 1938-1945. DOI: 10.1134/s1070363221100030
22. Serra, P. B. P. Thermal behaviour and heat capacity of ionic liquids: benzilimidazolium and alkylimidazolium derivatives M.Sc. Thesis, Universidade do Porto, 2013.
23. Serra, P.B.P.; Ribeiro, F.M.S.; Rocha, M.A.A.; Fulem, M.; Růžička, K.; Coutinho, J.A.P.; Santos, L.M.N.B.F. Solid-liquid equilibrium and heat capacity trend in the alkylimidazolium PF6 series *J. Mol. Liq*. **2017**, *248*, 678-687. DOI: 10.1016/j.molliq.2017.10.042.
24. Holbrey, J. D.; Reichert, W. M.; Reddy, R. G.; Rogers, R. D. Heat Capacities of Ionic Liquids and Their Applications as Thermal Fluids. In *Ionic Liquids as Green Solvents*. American Chemical Society: Washington D. C., 2003; Volume 856, Ch. 11, pp. 121-133 DOI: 10.1021/bk-2003-0856.ch011
25. Glasser, L.; Jenkins, H. D. B. Predictive thermodynamics for ionic solids and liquids *Phys. Chem. Chem. Phys*. **2016**, *18*, 21226. DOI: 10.1039/c6cp00235h
26. Fuller, J.; Carlin, R.T.; De Long, H.C.; Haworth, D. Structure of 1-ethyl-3-methylimidazolium hexafluorophosphate: model for room temperature molten salts *J. Chem. Soc., Chem. Commun*. **1994**, *3*, 299-300. DOI: 10.1039/C39940000299
27. Belov, G.V.; Iorish, V.S.; Yungman, V.S. IVTANTHERMO for Windows – database on thermodynamic properties and related software *CALPHAD: Comput. Coupling Phase Diagrams Thermochem*. **1999**, *23*, 173-180. DOI: 10.1016/S0364-5916(99)00023-1
28. Lemmon, E. W.; McLinden, M. O.; Friend, D. G. NIST Chemistry WebBook, NIST Standard Reference Database, **2017**. DOI: 10.18434/T4D303
29. Acree, W. Jr.; Chickos, J.S. Phase Transition Enthalpy Measurements of Organic and Organometallic Compounds. Sublimation, Vaporization and Fusion Enthalpies From 1880 to 2015. Part 1. C1 − C10 *J. Phys. Chem. Ref. Data*. **2016**, *45*, 033101 DOI: 10.1063/1.4948363
30. Zaitsau, D.H.; Kabo, G.J.; Strechan, A.A.; Paulechka, Y.U.; Tschersich, A.; Verevkin, S. P.; and Heintz, A. Experimental Vapor Pressures of 1-Alkyl-3-methylimidazolium Bis(trifluoromethylsulfonyl)imides and a Correlation Scheme for Estimation of Vaporization Enthalpies of Ionic Liquids *J. Phys. Chem. A*. **2006**, *110 (22)*, 7303-7306. DOI: 10.1021/jp060896f